Hindawi Publishing Corporation
Modelling and Simulation in Engineering
Volume 2016, Article ID 9453649, 11 pages
http://dx.doi.org/10.1155/2016/9453649

Research Article

Development of Constitutive Model for Precast Prestressed Concrete Segmental Columns

M. Hafezolghorani Esfahani,[1] F. Hejazi,[1] R. Vaghei,[1] E. Nikbakht,[2] and D. C. J. Tze[1]

[1]*Department of Civil Engineering, University of Putra Malaysia, Serdang, Malaysia*
[2]*Department of Civil Engineering, Universiti Teknologi Petronas, Malaysia*

Correspondence should be addressed to F. Hejazi; farzad@fhejazi.com

Received 1 December 2015; Accepted 28 February 2016

Academic Editor: Anna Pandolfi

The interest of using precast segmental columns in construction of concrete bridges has significantly increased in recent years. One research area of concrete bridges is the application of Precast Prestressed Concrete Segmental (PPCS) Column in any structural analysis software or FE program code. Modeling a PPCS column, which consists of various materials with interaction between them, is complicated and time-consuming. This research attempts to formulate the stiffness matrix of PPCS columns in order to form the constitutive model in linear form to evaluate the response of the columns. A two-dimensional finite element model is presented in the finite element package ANSYS. Parametric studies are conducted by finite element models to verify the constitutive models for the PPCS column with a different number of concrete segments. Comparison between the constitutive model and the FE program results indicates that the constitutive model is accurate enough to predict the deformation of the PPCS columns.

1. Introduction

Construction of segmental bridge started in Europe in 1950. The first attempt of cast-in-place segmental concrete bridge was conducted across the Lahn River in Balduinstein, Germany, in 1950; however, the primary precast segmental concrete bridge was constructed in 1962, across the River Seine in France. Later, this construction method gained worldwide recognition. Bridge construction time, facilitating construction, and minimizing the traffic disruption are the main advantages of precast construction in contrast to cast-in-situ construction. Precast segmental concrete bridges are normally constructed in low seismic areas. Numerous precast segmental concrete columns and pier constructions have been carried out in the US in low seismic regions such as the states of Texas and California in the United States [1]. Studies of PPCS column can be categorized into two parts: firstly, with bonded and, secondly, with unbounded posttensioning systems.

Different researchers presented various aspects of prestressing with bonded tendons in their research [2, 3]. In bonded posttensioned systems, the lateral strength of columns could be enhanced by the bonding between prestressing strands and surrounding concrete; however, it might result in tendon yielding. To the best of our knowledge, there are just a few studies in the literature about unbounded tendons [4, 5]. Unbounded posttensioned steels might lead to reduced prestress loss during strong seismic excitations. The segmental column can be restored to its original configuration after earthquakes, which cannot be done for bonded structure. It also maintains the continuity between column segments and foundation. There are several components in precast segmental bridge columns, which are combined and associated with continuous posttensioning strands. The action of these types of bridges against seismic loading differs from conventional bridge columns; besides, segmental bridges act with rocking mechanism, which takes place while the segments opening is to be found, and, as a consequence, the resultant damage is much lower than that in the conventional monolithic bridge columns. The minor cracks and damage in this system make them more economical than the monolithic system due to the reparability of this system after severe earthquake loading. The PRESS program has been established (Precast Seismic Structural Systems) as an

innovative alternative solution for precast connections by using prestressing strands and mild steel, in order to indicate appropriate ductility compared to conventional monolithic systems [6].

Prestressing strands have the capability of recentering against earthquake, which means they return the columns at the original place over the unloading stages. The mild steel reinforcements are able to dissipate the earthquake energy. The concept of a hybrid system has been introduced for the first time and applied for posttensioning in beam-column connections [7]. They claimed that the combination of prestressing strands and mild steel reinforcements can appropriately meet the design codes' requirements. Mild steel reinforcement and posttensioned tendons have an influential role in the ductility and strength of hybrid segmental systems due to their combination [8]. The performance of unbonded posttensioned prefabricated concrete segmental bridge column subjected to lateral earthquake loading has been analytically and experimentally investigated for four precast posttensioned columns with different thickness of steel jackets and the results indicated that these types of bridge columns have appropriate performance against seismic energy with negligible residual displacement. New criteria for functional and survival limits for posttensioned (PT) precast segmental bridge columns have been proposed [9]. At the functional level of earthquake, the objective is to keep the structure operational without occurrence of major damage while, at the survival limit, the objective is to prevent the structure from collapsing. They defined three criteria for the functionality of structure. First limit is yielding of the prestressing strands. The second criterion is the displacement which leads to 1% residual drift, and the third limit is 0.7 times the survival-level displacement. The surviving-level limit is the displacement at which the structure starts to collapse. Reduction of longitudinal reinforcements and increase in axial load result in minimal residual displacement [10]. Reduction by 86% in the residual displacement can be captured by replacing half of the rebar with prestressing strands and applying prestressing force that is equivalent to axial load due to dead load. They also investigated the dynamic analysis of the unbounded center strand columns. A combination ratio of energy dissipation of mild steel internal and/or external supplemental energy dissipation and self-centering posttensioning strands as one of the predominant design factors in hybrid posttensioned bridges has been proposed to achieve appropriate energy dissipation and self-centering capability with less damage and residual displacement against seismic loading [11, 12]. They used two rotational springs: one representing the behavior of prestressed tendons without the contribution of mild steel reinforcement, and the other representing only the mild steel reinforcement contribution. They investigated five specimens with different combination ratios. The experimental results proved the advantages of enhanced performance of the hybrid system in comparison with traditional monolithic solutions. The proposed hybrid system is shown to have minor flexural cracking, negligible residual displacement, and a stable hysteretic behavior up to high ductility level, so a combination ratio of prestressing strands and mild steel reinforcements in design is proposed. Some researchers have also investigated the behavior of hollow unbonded precast segmental bridge columns with rectangular box cross section, in which the prestressing strands were passed through the hollow ducts [12].

The actual simplicity at design and construction phase of high performance and low-cost hybrid bridge piers were studied by some researchers [13]. They also applied short lengths of unbonded mild steel reinforcements at the junction of footing-first segment to prevent premature yielding of longitudinal reinforcements. They indicated that a certain amount of unbonded length of mild reinforcements provides more energy dissipation and strength against earthquake loading. Furthermore, they claimed that the unbonded precast column could return to the undeformed position after earthquakes. Eight large-scale posttensioned precast columns were carried out to validate the detailed finite element model subjected to cyclic tests which was developed by ABAQUS platform, and the outcomes showed a good agreement [14]. A 3D finite element model of precast walls and connection was developed using finite element model [15]. A numerical analytical model with nonlinear factors of prestressing precast concrete bridge column systems, which consists of a segment model, prestressing tendon, and joint mode, was developed [16]. The detailed finite element model of prestressing bridge column was carried out with the structural analysis software "Open Sees" and, finally, the finite element outcomes met the experimental results. The monotonic behavior of precast segmental bridge columns has been investigated through three-dimensional finite element models [17, 18]. Later, they studied the accuracy of analytical results for predicting the damage when subjected to lateral loading. They also investigated the effects of posttensioning forces, the amount of segments, and aspect ratio (the relation between the heights of the column and the diameter of the column). Two types of numerical models for unbonded posttensioned (PT) precast concrete segmental bridge were presented by the computer program PISA [19]. A 3D nonlinear finite element model has been proposed for hybrid posttensioned precast segmental bridge columns to analyse the different prestressing strand levels subjected to nonlinear static and lateral seismic loading [20, 21].

Modeling a PPCS column with various materials and interaction has been studied by finite element model (FEM); however, the results show that this methodology is complicated and time-consuming. This paper presents the stiffness matrix of unbonded prestressed precast segmental (PPCS) column to form the constitutive model. Finite element formulations are derived in explicit form which is applicable in any structural analysis software or FEM program code. Finally, three finite element models of Precast Prestressed Concrete Segmental (PPCS) Column with respect to one, two, and three segments called RC1SS, RC2SS, and RC3SS are investigated.

2. Precast Prestressed Concrete Segmental Column

2.1. Description of the Case Study and Material Properties. Various experiments on different large-scale specimens have

Table 1: Material properties.

Concrete	Grade 40	$E_c = 30241$ MPa $\nu = 0.2$	$f_{cu} = 41.4$ MPa $f_t = 4.053$ MPa
Reinforcement	Grade 60	$E_s = 200000$ MPa	$f_{ys} = 410$ MPa
Prestressing steel	Grade 270	$E_p = 196500$ MPa	$f_{yp} = 1860$ MPa

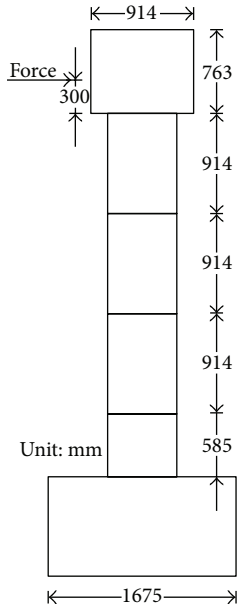

Figure 1: Geometry of the studied specimen [4].

been carried out in 2002 [4]. This study is chosen to develop the constitutive model. The geometry of the studied specimen is shown in Figure 1. Due to plane stress and plane strain analysis, two-dimensional view of the studied specimen has been chosen and equivalent section area is considered for 2D FE modeling and analysis.

The material properties of the specimens are presented in Table 1.

2.2. Constitutive Stress-Strain Relationships. Concrete is a quasi-brittle material which means concrete behaves differently against compression and tension. In general, concrete's tensile strength is only about 8% to 15% of the compressive strength. As shown in Figure 2(a), a stress-strain curve for confined concrete is presented in which f_c and f_{cu} are the peak compressive and ultimate strengths and ε_0 and ε_{cu} are the corresponding strains, respectively [22].

Idealized nonlinear prestressing steel with stress-strain model for 7-wire low-relaxation prestressing strand from ASTM A722 was proposed [4]. The curve, which is shown in Figure 2(b), can be derived by

prestress steel limit of proportionality: $\varepsilon_{lp} = 0.0086$,

reduced ultimate prestress steel strain: $\varepsilon_{lp} = 0.0300$,

$$\varepsilon_p \le 0.0086 : f_p = 28,500\varepsilon_p,$$
$$\varepsilon_p \ge 0.0086 : f_p = 270 - \frac{0.04}{\varepsilon_p - 0.007}. \quad (1)$$

Although the developed constitutive law is applicable for both linear and nonlinear analysis, linear analysis has been used in this paper to codify the finite element program due to its simplicity of application and verification.

3. Development of Constitutive Law

The proposed constitutive model for precast segmental columns comprises two stiffness matrixes for concrete and reinforcement. Each concrete segmental is modeled as two 4-node isoparametric elements as shown in Figure 3.

The shape function for isoparametric 4-node element is shown in Figure 4.

The displacement (u, v) is assumed as a bilinear function over the element and is given by the following [23]:

$$u = N_1u_1 + N_2u_2 + N_3u_3 + N_4u_4,$$
$$v = N_1v_1 + N_2v_2 + N_3v_3 + N_4v_4. \quad (2)$$

Element stiffness matrix is given as follows:

$$[k_c] = \int [B]^T [D] [B] \, dv = \iint_{-1}^{1} [B]^T [D] [B] \, t \, |J| \, d\xi \, d\eta, \quad (3)$$

where

$$dXdY = |J| \, d\xi d\eta,$$

$$D = \frac{E_c}{(1-\nu^2)} \begin{bmatrix} 1 & \nu & 0 \\ \nu & 1 & 0 \\ 0 & 0 & \frac{1}{2}(1-\nu) \end{bmatrix}$$

D matrix $\longrightarrow$ plane Stress, (4)

$$D = \frac{E_c}{(1+\nu)(1-2\nu)} \begin{bmatrix} 1-\nu & \nu & 0 \\ \nu & 1-\nu & 0 \\ 0 & 0 & \frac{1}{2}-\nu \end{bmatrix}$$

D matrix $\longrightarrow$ plane Strain.

The matrix J is known in mathematics as the Jacobian matrix and can be numerically evaluated from

$$[J] = \begin{bmatrix} \frac{\partial x}{\partial \xi} & \frac{\partial y}{\partial \xi} \\ \frac{\partial x}{\partial \eta} & \frac{\partial y}{\partial \eta} \end{bmatrix} = \begin{bmatrix} J_{11} & J_{12} \\ J_{21} & J_{22} \end{bmatrix}. \quad (5)$$

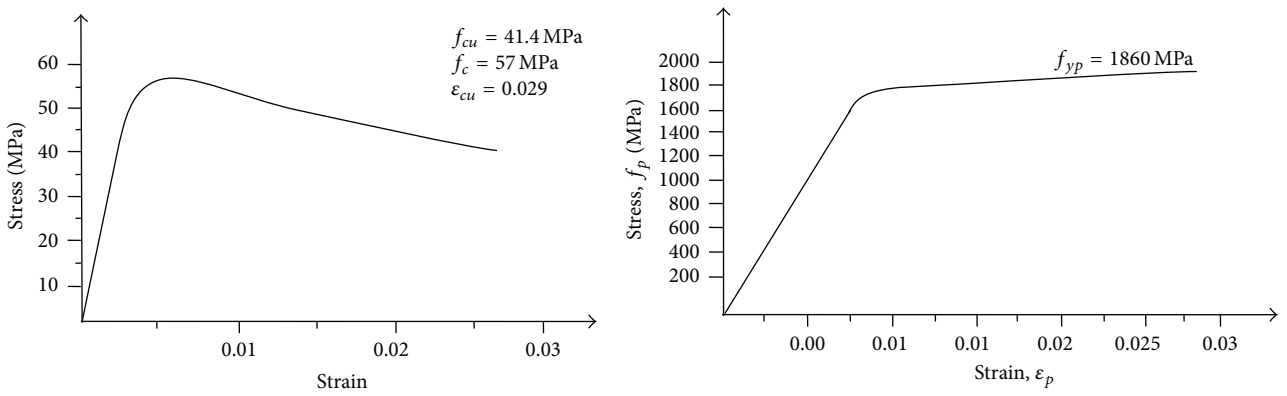

(a) Confined concrete (b) Prestressing steel

Figure 2: Stress-strain curves for materials [4, 22].

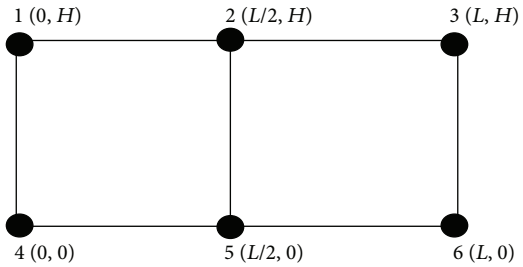

Figure 3: Modeling of concrete element.

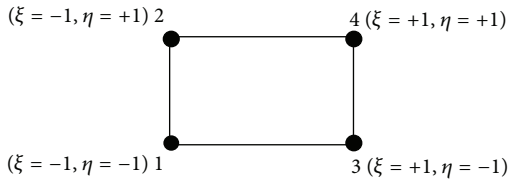

Figure 4: Shape function of isoparametric four nodes.

The force-displacement relation can be evaluated by

$$F = kd. \tag{6}$$

The strain-displacement relation is given by

$$\varepsilon = Bd. \tag{7}$$

The stress-strain relation can be obtained by

$$\sigma = D\varepsilon. \tag{8}$$

The discontinuous longitudinal reinforcement bar in the concrete segments and tendons is modeled as two (2) nodded bar elements. Each node of the truss is laterally restrained to the adjacent node of segmented column. The shape function of reinforcement bar is evaluated as shown in Figure 5.

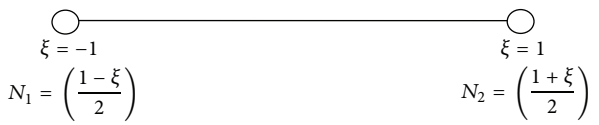

Figure 5: Shape function of bar element.

The stiffness matrix of reinforcement can be obtained by

$$\begin{aligned}[k_s] &= \int [B]^T [D] [B]\, dv = \int_l [B]^T [D] [B] A\, dx \\ &= \int_l [B]^T [D] [B] A |J|\, d\xi,\end{aligned} \tag{9}$$

where

$$dX = |J|\, d\xi. \tag{10}$$

It is known as

$$\begin{aligned}\frac{\partial N_i}{\partial x} &= \left[\frac{\partial x}{\partial \xi}\right]^{-1} \times \frac{\partial N_i}{\partial \xi}, \\ J &= \frac{\partial x}{\partial \xi}.\end{aligned} \tag{11}$$

Generally, the global stiffness of prestressed column in this study is formulated by assembling stiffness matrix for each concrete segment, prestressing tendon, longitudinal bar, and interface element.

4. Comparison of the Proposed Constitutive Model and FE Model

The contribution of tendons in precast concrete segments is investigated and new constitutive model is proposed and verified through modeling in FE software ANSYS.

Solution of many engineering problems is based on linear approximations and in this study the linear response is considered, although developed constitutive law is applicable for nonlinear analysis as well.

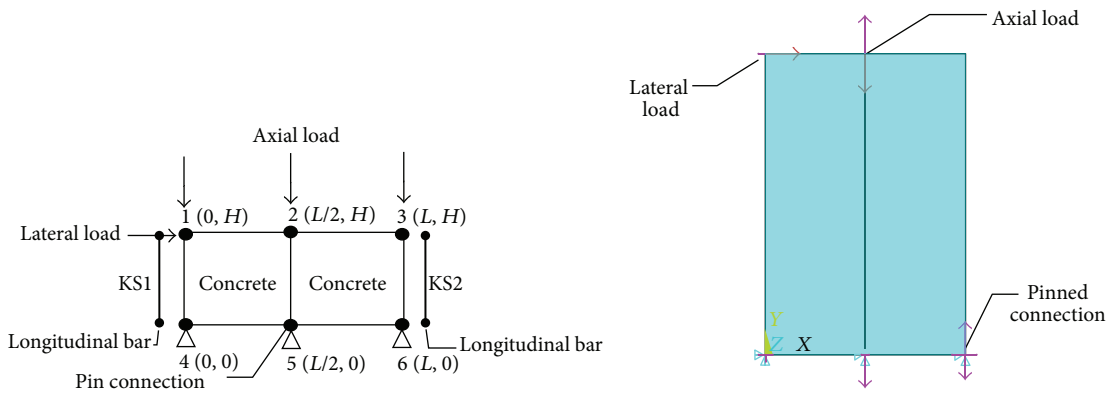

(a) Proposed constitutive model (b) FE model

FIGURE 6: One concrete segment model (RC1SS).

4.1. One Concrete Segment. Figure 6(a) shows the constitutive model of one concrete segment, where the longitudinal bars (KS1, KS2) are separated into sections equally and placed at both sides of the concrete segment; that is, KS1 is sharing node 1 and node 4 with the concrete segment in y direction while KS2 is sharing node 3 and node 6. The length of the longitudinal bar is the same as the height of single concrete segment. The lateral load is applied at node 1 of concrete segment with load step of 100 kN up to 500 kN and 500 kN is vertically and equally applied at top nodes (i.e., 1, 2, and 3). Figure 6(b) shows the finite element model for one concrete segment subjected to the lateral and axial loads.

The stiffness matrix for one concrete segment with longitudinal bar can be derived as shown in (12). The stiffness matrix variables A, B, C, a, b, c, d, e, f, and g are defined in Table 2.

A comparison between the constitutive model and FE model responses is carried out. As can be observed in Figure 7, it can be proven that the proposed constitutive model for one concrete segment has a good agreement with the FE model in plane stress analysis and plane strain analysis. As expected, displacement in plane strain analysis is about 80 mm which is four times higher than the displacement in plane stress analysis and both approaches show linear behavior:

$$K = C \times \begin{bmatrix} a & -c & -b & -d & 0 & 0 & b & d & -a & c & 0 & 0 \\ -c & e+g & d & f & 0 & 0 & -d & -f-g & c & -e & 0 & 0 \\ -b & d & 2a & 0 & -b & -d & -a & -c & 2b & 0 & -a & c \\ -d & f & 0 & 2e & d & f & -c & -e & 0 & -2b & c & -e \\ 0 & 0 & -b & d & a & c & 0 & 0 & -a & -c & b & -d \\ 0 & 0 & -d & f & c & e+g & 0 & 0 & -c & -e & d & -f-g \\ b & -d & -a & -c & 0 & 0 & a & c & -b & d & 0 & 0 \\ d & -f-g & -c & -e & 0 & 0 & c & e+g & -d & f & 0 & 0 \\ -a & c & 2b & 0 & -a & -c & -b & -d & 2a & 0 & -b & d \\ c & -e & 0 & -2b & -c & -e & d & f & 0 & 2e & -d & f \\ 0 & 0 & -a & c & b & d & 0 & 0 & -b & -d & a & -c \\ 0 & 0 & c & -e & -d & -f-g & 0 & 0 & d & f & -c & e+g \end{bmatrix}. \quad (12)$$

It can be seen from Table 3 that, in plane stress analysis, the maximum displacement by the proposed constitutive model is close to that obtained by FE model, with the former value a little bit more than the latter one. A maximum difference of 4.6% is observed between constitutive model and FE results. In plane strain analysis, the maximum displacement is 76.89 mm in the proposed constitutive model; however, the correspondence value in FE model is 73.94 mm. Table 3 shows about four percent difference in plane strain analysis between proposed constitutive model and FE results for one segmental concrete, whilst discrepancy percentage of aforementioned methods in plane stress analysis is increased to 4.6%.

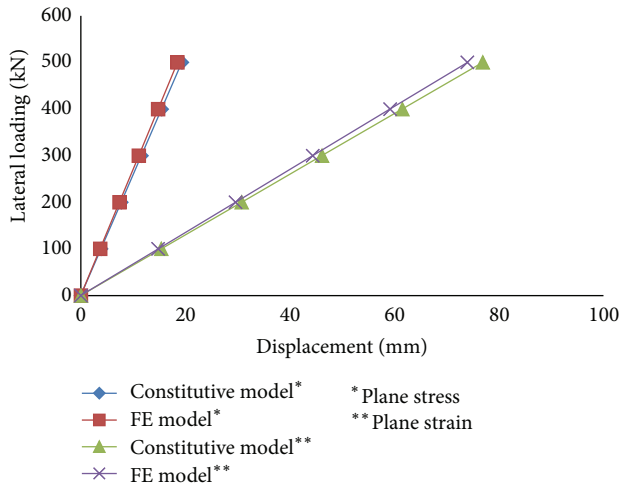

FIGURE 7: Lateral load-deflection of the proposed constitutive model and FE model for RC1SS.

4.2. Two Concrete Segments. Two concrete segments are attached together as shown in Figure 8(a) with prestressing tendon placed at the middle of the concrete segment, which connects node 2 and node 8 in order to connect the concrete segments together (RC2SS). The intention of designing longitudinal reinforcement discontinuously is to avoid the fracture of mild steel at the critical joint opening when a huge lateral load is applied. The developed constitutive model for RC2SS is examined under the following load condition as shown in Figure 8(b). The prestressing tendon role is to overcome weakness of concrete in tension by providing the clamping load between the concrete segment and support.

From (13), the stiffness matrix for the prestressing tendon can be derived as

$$[K_t] = \frac{E_t A_t}{H} \begin{matrix} \\ 8y \\ -1 \end{matrix} \begin{matrix} \begin{matrix} 2y \end{matrix} \\ \begin{bmatrix} 1 & -1 \\ -1 & 1 \end{bmatrix} \end{matrix},$$

$$t = \frac{E_t A_t}{H} \times \frac{8LH\left(1-\nu^2\right)}{Et} \quad \text{(plane stress)}, \tag{13}$$

$$t = \frac{E_t A_t}{H} \times \frac{16LH\left(1+\nu\right)B}{Et} \quad \text{(plane strain)}.$$

So by substituting these parameters in (14), the stiffness matrix can be derived as

$$K_2 = C \times \begin{bmatrix}
a & -c & -b & 0 & 0 & b & d & -a & 0 & 0 & 0 & 0 & 0 & 0 & 0 & 0 & 0 & 0 \\
-c & e+g & d & 0 & 0 & -d & -f-g & c & -e & 0 & 0 & 0 & 0 & 0 & 0 & 0 & 0 & 0 \\
-b & d & 2a & 0 & -b & -d & -a & -c & 2b & 0 & -a & c & 0 & 0 & 0 & 0 & 0 & 0 \\
-d & f & 0 & 2e+t & d & f & -c & -e & 0 & -2f & c & -e & 0 & 0 & 0 & -t & 0 & 0 \\
0 & 0 & -b & d & a & c & 0 & 0 & -a & -c & b & -d & 0 & 0 & 0 & 0 & 0 & 0 \\
0 & 0 & -d & f & c & e+g & 0 & 0 & -c & -e & d & -f-g & 0 & 0 & 0 & 0 & 0 & 0 \\
b & -d & -a & -c & 0 & 0 & 2a & 0 & -2b & 0 & 0 & 0 & b & d & -a & c & 0 & 0 \\
d & -f-g & -c & -e & 0 & 0 & 0 & 2(e+g) & 0 & 2f & 0 & 0 & -d & -f-g & c & -e & 0 & 0 \\
-a & c & 2b & 0 & -a & -c & -2b & 0 & 4a & 0 & -2b & 0 & -a & -c & 2b & 0 & -a & c \\
c & -e & 0 & -2f & -c & -e & 0 & 2f & 0 & 4e & 0 & 2f & -c & -e & 0 & -2f & c & -e \\
0 & 0 & -a & c & b & d & 0 & 0 & -2b & 0 & 2a & c & 0 & 0 & -a & -c & b & -d \\
0 & 0 & c & -e & -d & -f-g & 0 & 0 & 0 & 2f & c & 2(e+g) & 0 & 0 & -c & e & d & -f-g \\
0 & 0 & 0 & 0 & 0 & 0 & b & -d & -a & -c & 0 & 0 & a & c & -b & d & 0 & 0 \\
0 & 0 & 0 & 0 & 0 & 0 & d & -f-g & -c & -e & 0 & 0 & c & e+g & -d & f & 0 & 0 \\
0 & 0 & 0 & 0 & 0 & 0 & -a & c & 2b & 0 & -a & -c & -b & -d & 2a & 0 & -b & d \\
0 & 0 & 0 & -t & 0 & 0 & c & -e & 0 & -2f & -c & -e & d & f & 0 & 2e+t & -d & f \\
0 & 0 & 0 & 0 & 0 & 0 & 0 & 0 & -a & c & b & d & 0 & 0 & -b & -d & a & -c \\
0 & 0 & 0 & 0 & 0 & 0 & 0 & 0 & c & -e & -d & -f-g & 0 & 0 & d & f & -c & e+g
\end{bmatrix}. \tag{14}$$

Comparison between the constitutive and FE models for two concrete segments, RC2SS, is shown in Figure 9. From this figure, it can be seen that there is a good agreement between the proposed constitutive model results for RC2SS and the FE model results in plane stress and plane strain analysis. Consequently, it can be determined that the maximum displacement in plane strain analysis is about 200 mm, which is almost three times higher than the displacement in plane stress analysis. Linear behavior has been captured for both aforementioned approaches.

Table 2: Stiffness matrix variables.

Plane stress condition	Plane strain condition
$A = \frac{1}{2}(1-\nu)$	$B = (1-2\nu)$
$C = \frac{Et}{8LH(1-\nu^2)}$	$C = \frac{Et}{16LH(1+\nu)B}$
$a = 4H^2 + AL^2$	$a = 8H^2(1-\nu) + L^2(1-2\nu)$
$b = 4H^2 - AL^2$	$b = 8H^2(1-\nu) - L^2(1-2\nu)$
$c = 2HL(\nu + A)$	$c = 2HL$
$d = 2HL(\nu - A)$	$d = 2HL(4\nu - 1)$
$e = L^2 + 4H^2A$	$e = 2L^2(1-\nu) + 4H^2(1-2\nu)$
$f = L^2 - 4H^2A$	$f = 2L^2(1-\nu) - 4H^2(1-2\nu)$
$g = \frac{E_sA_s}{2H} \times \frac{8LH(1-\nu^2)}{Et}$	$g = \frac{E_sA_s}{2H} \times \frac{16LH(1+\nu)B}{Et}$

Table 4 represents the percentage difference between two types of analysis on two concrete segments. In plane stress analysis, maximum displacements of 74.46 mm for the proposed constitutive model and 73.94 mm in FE program are achieved subjected to applied load. Likewise, in plane strain analysis, applied forces produce 191.21 mm and 194.19 mm displacements by proposed constitutive model and FE model, respectively. Table 4 shows almost 0.65% difference between two approaches in plane stress analysis for different applied load; however, this percentage difference in plane strain analysis for two concrete segments is diminished from 6.73% to 1.53% owing to the applied load from 100 kN to 500 kN as a lateral load and 500 kN as a vertical load.

4.3. Three Concrete Segments. The PPCS column consisting of three concrete segments is shown in Figure 10(a). The constitutive model has 12 nodes where each node has two degrees of freedom and resulting stiffness matrix size is 24 × 24. The prestressing tendons are pulled between node 2 and node 11. There are discontinuous bars at both sides of the concrete segment. The stiffness matrix for three segmental precast columns is developed by assembling the stiffness matrixes and presented by (15). Based on the developed constitutive model, the PPCS column with three concrete segments is modeled by only 15 elements which reduce computation time and convergence issues of analysis considerably.

The analysis result of RC3SS is plotted in Figure 11 and tabulated in Table 5. It is clear from these plots that the constitutive model has smaller displacement than the FE model. As can be observed in Figure 11, there is a good agreement between the proposed constitutive model and the FE model in plane stress and plane strain analysis of RC3SS. Consequently, it can be found that displacement in plane stress analysis is about 200 mm and it is almost doubled in plane strain:

$$K = \frac{Et}{8LH(1-\nu^2)} \cdot \begin{bmatrix}
2a & 0 & b & -d & -2b & 0 & -a & -c & 0 & 0 & 0 & 0 & b & d & -a & c & 0 & 0 & 0 & 0 & 0 & 0 & 0 & 0 \\
0 & 2(e+g) & d & -f-g & 0 & 2f & -c & -e & 0 & 0 & 0 & 0 & -d & -f-g & c & -e & 0 & 0 & 0 & 0 & 0 & 0 & 0 & 0 \\
b & d & a & -c & -a & c & -b & -d & 0 & 0 & 0 & 0 & 0 & 0 & 0 & 0 & 0 & 0 & 0 & 0 & 0 & 0 & 0 & 0 \\
-d & -f-g & -c & e+g & c & -e & d & f & 0 & 0 & 0 & 0 & 0 & 0 & 0 & 0 & 0 & 0 & 0 & 0 & 0 & 0 & 0 & 0 \\
-2b & 0 & -a & c & 4a & 0 & 2b & 0 & -2b & 0 & -a & -c & -a & -c & 2b & 0 & -a & c & 0 & 0 & 0 & 0 & 0 & 0 \\
0 & 2f & c & -e & 0 & 4a & 0 & -2f & 0 & 2f & -c & -e & -c & -e & 0 & -2f & c & -e & 0 & 0 & 0 & 0 & 0 & 0 \\
-a & -c & -b & d & 2b & 0 & 2a & 0 & -a & c & -b & -d & 0 & 0 & 0 & 0 & 0 & 0 & 0 & 0 & 0 & 0 & 0 & 0 \\
-c & -e & -d & f & 0 & -2f & 0 & 2e+t & c & -e & d & f & 0 & 0 & 0 & 0 & 0 & 0 & 0 & 0 & 0 & -t & 0 & 0 \\
0 & 0 & 0 & 0 & -2b & 0 & -a & c & 2a & 0 & b & d & 0 & 0 & -a & -c & b & -d & 0 & 0 & 0 & 0 & 0 & 0 \\
0 & 0 & 0 & 0 & 0 & 2f & c & -e & 0 & 2(e+g) & -d & -f-g & 0 & 0 & -c & -e & d & -f-g & 0 & 0 & 0 & 0 & 0 & 0 \\
0 & 0 & 0 & 0 & -a & -c & -b & d & b & -d & a & c & 0 & 0 & 0 & 0 & 0 & 0 & 0 & 0 & 0 & 0 & 0 & 0 \\
0 & 0 & 0 & 0 & -c & -e & -d & f & d & -f-g & c & e+g & 0 & 0 & 0 & 0 & 0 & 0 & 0 & 0 & 0 & 0 & 0 & 0 \\
b & -d & 0 & 0 & -a & -c & 0 & 0 & 0 & 0 & 0 & 0 & 2a & 0 & -2b & 0 & 0 & 0 & b & d & -a & c & 0 & 0 \\
d & -f-g & 0 & 0 & -c & -e & 0 & 0 & 0 & 0 & 0 & 0 & 0 & 2(e+g) & 0 & 2f & 0 & 0 & -d & -f-g & c & -e & 0 & 0 \\
-a & c & 0 & 0 & 2b & 0 & 0 & 0 & -a & -c & 0 & 0 & -2b & 0 & 4a & 0 & -2b & 0 & -a & -c & 2b & 0 & -a & c \\
c & -e & 0 & 0 & 0 & -2f & 0 & 0 & -c & -e & 0 & 0 & 0 & 2f & 0 & 4e & 0 & 2f & -c & -e & 0 & -2f & c & -e \\
0 & 0 & 0 & 0 & -a & c & 0 & 0 & b & d & 0 & 0 & 0 & 0 & -2b & 0 & 2a & 0 & 0 & 0 & -a & -c & b & -d \\
0 & 0 & 0 & 0 & c & -e & 0 & 0 & -d & -f-g & 0 & 0 & 0 & 0 & 0 & 2f & 0 & 2(e+g) & 0 & 0 & -c & -e & d & -f-g \\
0 & 0 & 0 & 0 & 0 & 0 & 0 & 0 & 0 & 0 & 0 & 0 & b & -d & -a & -c & 0 & 0 & a & c & -b & d & 0 & 0 \\
0 & 0 & 0 & 0 & 0 & 0 & 0 & 0 & 0 & 0 & 0 & 0 & d & -f-g & -c & -e & 0 & 0 & c & e+g & -d & f & 0 & 0 \\
0 & 0 & 0 & 0 & 0 & 0 & 0 & 0 & 0 & 0 & 0 & 0 & -a & c & 2b & 0 & -a & -c & -b & -d & 2a & 0 & -b & d \\
0 & 0 & 0 & 0 & 0 & 0 & 0 & -t & 0 & 0 & 0 & 0 & c & -e & 0 & -2f & -c & -e & d & f & 0 & 2e+t & -d & f \\
0 & 0 & 0 & 0 & 0 & 0 & 0 & 0 & 0 & 0 & 0 & 0 & 0 & 0 & -a & c & b & d & 0 & 0 & -b & -d & a & -c \\
0 & 0 & 0 & 0 & 0 & 0 & 0 & 0 & 0 & 0 & 0 & 0 & 0 & 0 & c & -e & -d & -f-g & 0 & 0 & d & f & -c & e+g
\end{bmatrix}. \quad (15)$$

Table 3: Displacement comparison of the constitutive model and FE model of RC1SS at node 1.

Lateral load (kN)	Constitutive model (plane stress) (mm)	FE program (plane stress) (mm)	Percentage difference (plane stress) (%)	Constitutive model (plane strain) (mm)	FE program (plane strain) (mm)	Percentage difference (plane strain) (%)
0	0	0	—	0	0	—
100	3.88	3.70	4.60	15.38	14.78	4
200	7.73	7.39	4.60	30.75	29.57	4
300	11.60	11.09	4.60	46.13	44.37	4
400	15.47	14.79	4.60	61.51	59.15	4
500	19.33	18.49	4.60	76.89	73.94	4

Table 4: Displacement comparison of the constitutive model and FE model of RC2SS at node 1.

Lateral load (kN)	Constitutive model (plane stress) (mm)	FE program (plane stress) (mm)	Percentage difference (plane stress) (%)	Constitutive model (plane strain) (mm)	FE program (plane strain) (mm)	Percentage difference (plane strain) (%)
0	0	0	—	0	0	—
100	14.82	14.93	0.68	37.38	40.08	6.73
200	29.73	29.62	0.39	75.83	78.95	3.94
300	44.64	44.35	0.66	114.29	117.60	2.8
400	59.55	59.13	0.71	152.75	156.02	2.09
500	74.46	73.94	0.7	191.21	194.19	1.53

Table 5: Comparison of constitutive model and FE model for displacement of RC3SS at node 1.

Lateral load (kN)	Constitutive model (plane stress) (mm)	FE program (plane stress) (mm)	Percentage difference (plane stress) (%)	Constitutive model (plane strain) (mm)	FE program (plane strain) (mm)	Percentage difference (plane strain) (%)
0	0	0	—	0	0	—
100	41.19	42.28	2.57	78.17	84.28	7.24
200	82.15	84.57	2.86	155.77	167.52	7
300	123.11	127.11	3.14	233.37	250.49	6.83
400	164.06	169.82	3.39	310.98	332.98	6.60
500	205.02	212.69	3.60	388.58	414.78	6.31

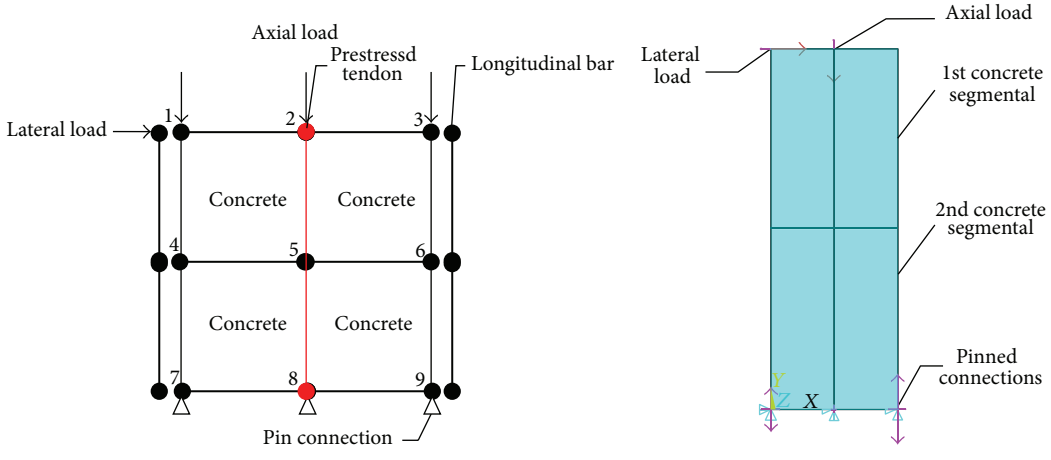

(a) Proposed constitutive model (b) FE model

Figure 8: Two concrete segments' model (RC2SS).

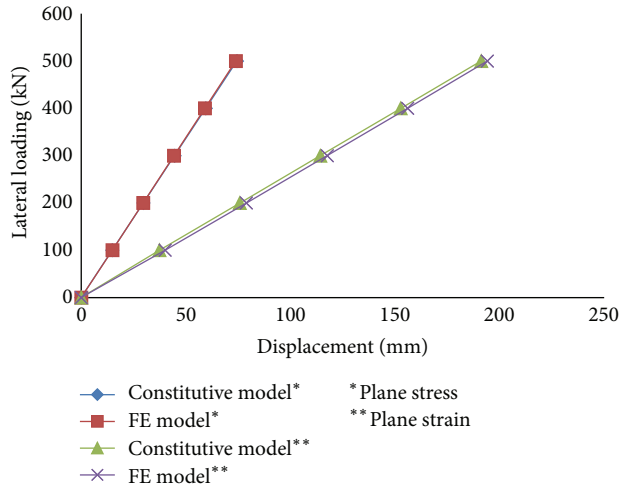

FIGURE 9: Lateral load-deflection of the proposed constitutive model and FE model for RC2SS.

A comparison between the constitutive model and FE model results is carried out under plane stress and plane strain analysis as shown in Table 5. The displacement increases clearly with applied load, for instance, in plane stress analysis; load applied is the same as in previous steps and results in 205.02 mm and 212.69 mm displacements in the proposed constitutive and FE models, respectively. Likewise, in plane strain analysis, applied force produces 388.58 mm and 414.78 mm displacements at node 1 in the proposed constitutive and FE models, respectively.

A maximum difference of 3.6% is observed between the results of the constitutive model and FE program for plane stress analysis of RC3SS model. Also, it can be seen that the constitutive model provides reasonable correlation with the FE program results under plane strain analysis for PPCS columns with three concrete segments.

Based on the outputs, it is clear from the plots that increasing the load increases the maximum displacement in plane stress or plane strain analysis. It can be determined that, in plane stress analysis with the proposed constitutive model, applying load incrementally up to 500 kN with 100 kN as each load step in a lateral direction and 500 kN as a vertical load results in almost 20 mm, 75 mm, and 200 mm as maximum displacements, which are close to the FEM results with about 4.6%, 0.7%, and 3.6% difference in one, two, and three concrete segments, respectively. Likewise, the proposed constitutive model in plane strain analysis shows about 77 mm, 191 mm, and 388 mm displacement in one, two, and three concrete segments subjected to imposed loading, while the FE program shows 74 mm and 194 mm to 414 mm as maximum displacements by 4%, 1.53%, and 6% difference, respectively.

Short-term stress losses may happen due to wobble and curvature frictions and anchorage slip. On the other hand, long-term stress losses include relaxation, elastic shortening, and losses due to creep, shrinkage, and superimposed loads.

Although in this study effects of losses are not considered, however, as a matter of fact, it can be easily incorporated into the stiffness matrix of prestress concrete particularly in elastic modulus of tendon and concrete individually as a degraded elastic modulus before forming global matrix (refer to (14) and (15)).

Short-term losses also could be considered in stiffness matrix of prestressed concrete element as a multiplayer of the yield stress of tendon which varies between 0.7 and 0.9. The effective strand strain after transfer is slightly overestimated because the model considered low-relaxation prestressing strand and does not take into account the long-term prestress losses due to concrete creep and shrinkage.

5. Conclusions

Modeling of PPCS column is not easy using available commercial software packages because all the parts should be modeled separately. Moreover, the interaction between different parts should be defined, which not only increases computation time but also requires experts.

In this study, an attempt was made to develop the constitutive model for PPCS columns in bridge structures. Moreover, FEM model for one, two, and three segments was developed in order to perform linear and nonlinear analysis for PPCS column subjected to static and dynamic loading.

A special FEM program was codified by using developed PPCS columns, and the accuracy of the developed constitutive model was evaluated by comparing analysis results with commercial software. Using this method would not only reduce modeling and computation time but also considerably facilitate the convergence problems due to diminishing meshing adaption issues by substituting meshing assemblage to one explicit matrix in which all characteristics of meshes are incorporated. The PPCS column is applicable as a supplementary subroutine in any structural analysis software or can be used to develop any FEM program code for analysis of PPCS columns.

Nomenclature

E: Young's modulus
E_c: Concrete Young's modulus
E_s: Steel Young's modulus
E_p: Prestressing steel Young's modulus
ν: Poisson's ratio
f_c: Stress of concrete in compression
f_t: Stress of concrete in tension
f_{ys}: Yield stress of reinforcing bar
f_{yp}: Yield stress of prestressing steel
f_{cu}: Ultimate compressive strength of concrete
k_c: Stiffness matrix of concrete
k_s: Stiffness matrix of reinforcing bar
k_t: Stiffness matrix of prestressing steel
B: Strain-displacement matrix
D: Constitutive matrix
N: Shape function
J: Jacobian matrix
ε_{lp}: Prestress steel limit
ε_p: Strain of prestressing steel
ξ: Natural coordinate.

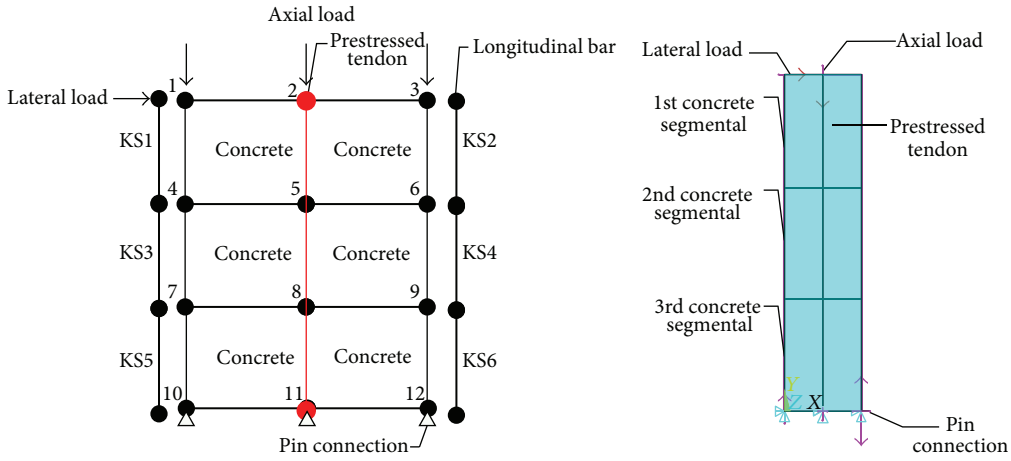

(a) Proposed constitutive model (b) FE model

Figure 10: Three concrete segments' model (RC3SS).

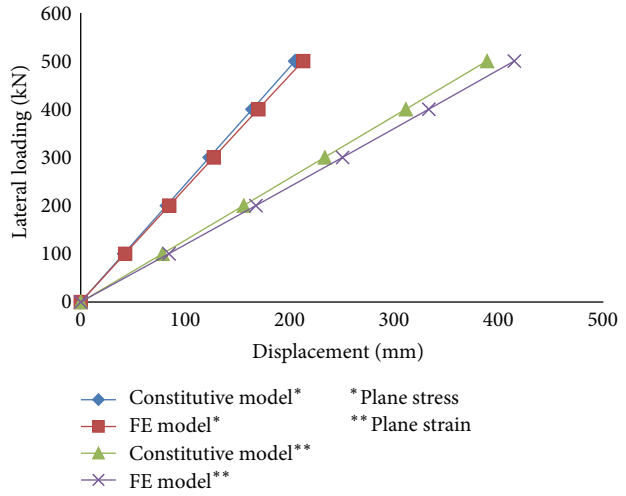

Figure 11: Lateral load-deflection of the proposed constitutive model and FE model for RC3SS.

Competing Interests

The authors declare that there are no competing interests regarding the publication of this paper.

Acknowledgments

This work received financial support from the Ministry of Higher Education of Malaysia under FRGS Research Projects no. 5524254 and no. 5524256 and was further supported by the University Putra Malaysia under Putra Grant no. 9415100. These supports are gratefully acknowledged.

References

[1] Y.-C. Ou, M. Chiewanichakorn, A. J. Aref, and G. C. Lee, "Seismic performance of segmental precast unbonded posttensioned concrete bridge columns," *Journal of Structural Engineering*, vol. 133, no. 11, pp. 1636–1647, 2007.

[2] K. Chang, C. H. Loh, H. S. Chiu et al., *Seismic Behavior of Precast Segmental Bridge Columns and Design Methodology for Applications in Taiwan*, Taiwan Area National Expressway Engineering Bureau, Taipei, Taiwan, 2002 (Chinese).

[3] T.-H. Kim, H.-M. Lee, Y.-J. Kim, and H. M. Shin, "Performance assessment of precast concrete segmental bridge columns with a shear resistant connecting structure," *Engineering Structures*, vol. 32, no. 5, pp. 1292–1303, 2010.

[4] J. T. Hewes and M. N. Priestley, *Seismic Design and Performance of Precast Concrete Segmental Bridge Columns*, University of California, Oakland, Calif, USA, 2002.

[5] S. L. Billington and J. K. Yoon, "Cyclic response of unbonded posttensioned precast columns with ductile fiber-reinforced concrete," *Journal of Bridge Engineering*, vol. 9, no. 4, pp. 353–363, 2004.

[6] M. J. Nigel Priestley, "Overview of PRESSS research program," *PCI Journal*, vol. 36, no. 4, pp. 50–57, 1991.

[7] W. C. Stone, G. S. Cheok, and J. F. Stanton, "Performance of hybrid moment-resisting precast beam-column concrete connections subjected to cyclic loading," *ACI Structural Journal*, vol. 92, no. 2, pp. 229–249, 1995.

[8] Y. Wang, Z. Y. Bu, and L. Hu, "Seismic behavior of precast segmental bridge columns with carbon fibre reinforcement as energy dissipation bars," *Applied Mechanics and Materials*, vol. 157, pp. 1148–1152, 2012.

[9] W.-P. Kwan and S. L. Billington, "Unbonded posttensioned concrete bridge piers. II. Seismic analyses," *Journal of Bridge Engineering*, vol. 8, no. 2, pp. 102–111, 2003.

[10] J. Sakai and S. A. Mahin, *Analytical Investigations of New Methods for Reducing Residual Displacements of Reinforced Concrete Bridge Columns*, Pacific Earthquake Engineering Research Center, University of California at Berkeley, Berkeley, Calif, USA, 2004.

[11] A. Palermo, S. Pampanin, and G. M. Calvi, "Concept and development of hybrid solutions for seismic resistant bridge systems," *Journal of Earthquake Engineering*, vol. 9, no. 6, pp. 899–921, 2005.

[12] Y.-C. Ou, M.-S. Tsai, K.-C. Chang, and G. C. Lee, "Cyclic behavior of precast segmental concrete bridge columns with high performance or conventional steel reinforcing bars as energy dissipation bars," *Earthquake Engineering & Structural Dynamics*, vol. 39, no. 11, pp. 1181–1198, 2010.

[13] A. Palermo, S. Pampanin, and D. Marriott, "Design, modeling, and experimental response of seismic resistant bridge piers with posttensioned dissipating connections," *Journal of Structural Engineering*, vol. 133, no. 11, pp. 1648–1661, 2007.

[14] M. A. Elgawady and A. Sha'Lan, "Seismic behavior of self-centering precast segmental bridge bents," *Journal of Bridge Engineering*, vol. 16, no. 3, pp. 328–339, 2011.

[15] R. Vaghei, F. Hejazi, H. Taheri, M. S. Jaafar, and A. A. Ali, "Evaluate performance of precast concrete wall to wall connection," *APCBEE Procedia*, vol. 9, pp. 285–290, 2014.

[16] Z. Wang, W. Song, Y. Wang, and H. Wei, "Numerical analytical model for seismic behavior of prestressing concrete bridge column systems," *Procedia Engineering*, vol. 14, pp. 2333–2340, 2011.

[17] H. Dawood, M. ElGawady, and J. Hewes, "Behavior of segmental precast posttensioned bridge piers under lateral loads," *Journal of Bridge Engineering*, vol. 17, no. 5, pp. 735–746, 2012.

[18] Z.-Y. Bu and Y.-C. Ou, "Simplified analytical pushover method for precast segmental concrete bridge columns," *Advances in Structural Engineering*, vol. 16, no. 5, pp. 805–822, 2013.

[19] C.-C. Chou, H.-J. Chang, and J. T. Hewes, "Two-plastic-hinge and two dimensional finite element models for post-tensioned precast concrete segmental bridge columns," *Engineering Structures*, vol. 46, pp. 205–217, 2013.

[20] E. Nikbakht, K. Rashid, F. Hejazi, and S. A. Osman, "A numerical study on seismic response of self-centring precast segmental columns at different post-tensioning forces," *Latin American Journal of Solids and Structures*, vol. 11, no. 5, pp. 864–883, 2013.

[21] E. Nikbakht, K. Rashid, F. Hejazi, and S. A. Osman, "Application of shape memory alloy bars in self-centring precast segmental columns as seismic resistance," *Structure and Infrastructure Engineering*, vol. 11, no. 3, pp. 297–309, 2015.

[22] J. B. Mander, M. J. Priestley, and R. Park, "Theoretical stress-strain model for confined concrete," *Journal of Structural Engineering*, vol. 114, no. 8, pp. 1804–1826, 1988.

[23] G. Strang and G. J. Fix, *An Analysis of the Finite Element Method*, Prentice-Hall, Englewood Cliffs, NJ, USA, 1973.